Dielectric Properties and Phase Stabilization of PVDF Polymer in (1−x) PVDF/xBCZT Composite Films

Tarun Garg[1,2,3] · Venkateswarlu Annapureddy[4] · K. C. Sekhar[5] · Dae-Yong Jeong[6] · Navneet Dabra[7] · Jasbir S. Hundal[2]

Abstract

Polyvinylidene fluoride (PVDF) is a semi-crystalline ferroelectric polymer which can be stabilized in its distinct electroactive polymorphs α and γ by selective processing techniques. In this article, to study the effect of processing temperature and barium calcium zirconium titanate (BCZT) ceramic-doping on PVDF phase stabilization, the pure PVDF and PVDF/BCZT composite films were fabricated by solution-casting and melt-pressing. The Fourier-transform infrared spectroscopy and x-ray diffraction studies showed that the pure PVDF and PVDF/BCZT composite films fabricated by solution-casting possessed the characteristic γ-PVDF peaks while melt-pressing stabilized PVDF mostly in the α-phase. The BCZT ceramic particles were found to have no significant effect on PVDF phase stabilization, but it enhanced the overall crystallinity of polymer matrix. The dielectric studies revealed that the relative permittivity (ε_r) of γ- and α-PVDF phases in pure PVDF film samples was ≈ 10 and 7.5 (at 120 Hz) respectively. The ε_r of PVDF/BCZT composite films having 50 wt.% BCZT content synthesized by solution-casting and melt-pressing were estimated to be ≈ 31 and 20 (at 120 Hz), respectively, which was about three times that of pure PVDF film synthesized by the respective technique. The value of loss tangent (tanδ) for pure PVDF films synthesized by solution-cast and melt-press technique were ≈ 0.07 and 0.35 (at 120 Hz) respectively. In temperature-dependent dielectric studies, γ-PVDF showed distinct α-relaxation peak at ≈ 120°C and polymer melting at temperature > 130°C. For α-PVDF, the increase in ε_r and tanδ was observed during α-relaxation transition at higher temperatures. The dielectric studies indicated that the introduction of BCZT ceramic particles in PVDF matrix increased the ε_r-value by enhancing the dipolar and interfacial polarizations in composites, while the decrease in tanδ-value was observed due to decrease in molecular dipoles with a decrease in wt.% of PVDF content. These phenomena collectively improved the overall electric properties of ceramic/polymer composites which makes them suitable candidates to explore for flexible electroactive material form.

Keywords Polyvinylidene fluoride (PVDF) · Barium calcium zirconium titanate (BCZT) · composite film · solution-casting · melt-pressing · FTIR · XRD · dielectric properties

✉ Navneet Dabra
  navneetdabra@gmail.com

1   Research Scholar, I. K. Gujral Punjab Technical University, Jalandhar-Kapurthala Highway, Kapurthala, Punjab 144603, India

2   Ferroelectric Materials Laboratory, Department of Physics, Maharaja Ranjit Singh Punjab Technical University, Bathinda, Punjab 151001, India

3   Punjabi University Guru Kashi College, Damdama Sahib, Talwandi Sabo, Punjab 151302, India

4   Department of Physics, National Institute of Technology, Tiruchirappalli, Tamil Nadu 620015, India

5   Department of Physics, School of Basic and Applied Sciences, Central University of Tamil Nadu, Thiruvarur, Tamil Nadu 610005, India

6   Department of Materials Science and Engineering, Inha University, Post No. 22212, Incheon 402751, Korea

7   Mata Sahib Kaur Girls College, Damdama Sahib, Talwandi Sabo, Punjab 151302, India

Introduction

Polyvinylidene fluoride (PVDF) is a semi-crystalline multiphase ferro/piezoelectric polymer.[1–4] It can be stabilized in its distinct polymorphs, α (TGTG′, form II), β (TTTT, form I), γ (T_3GT_3G', form III), δ and ε depending on the molecular chain conformation during the fabrication process.[3,5–10] Various techniques and treatments such as mechanical (stretching),[11,12] thermal (heat temperature),[13] electrical (poling process)[14] and chemical treatments (effect of solvents or other additives)[9,15–19] during the processing of PVDF affect the molecular phase stabilization in it and hence, the final properties. Among its all forms, β-PVDF is the most electroactive showing good ferro/piezoelectric properties.[2–4,10,16,20–23] However, the α- and γ-phases of PVDF are the most explored for applications in dielectric energy storage capacitors due to their low remnant polarization (P_r) value.[24] Obtaining PVDF in these phases by chemical treatments is found to be an effective and convenient methodology due to its ease of control, low haze and low processing temperature requirements.[4,9,18,25–27] Moreover, in general, the sol-gel techniques involve softer synthesis conditions during processing which further affect the properties of the final material form.[25,26,28] The recent research work in the development of electroactive polymers, particularly on PVDF, has reported the effect of various additives and techniques involved in phase stabilization to obtain enhanced electric properties.[6,7,10,15,18,23,29–33] In this article, the PVDF films were fabricated by solution-casting and melt-pressing which involved different methodologies and processing temperatures during fabrication. PVDF, being a typical engineering polymer material, possesses outstanding ferro/piezo/pyroelectric properties, high dielectric breakdown strength, better chemical, mechanical and thermal stability, and biocompatibility which makes it a suitable candidate for application in flexible memory, energy transducers, self-charging energy storage capacitors, sensors and electronic bio-medical devices.[2–4,6,10,18,20,22,30–32,34,35] However, with the progress in the field of electronics and electric industries, the single-phase polymer materials cannot meet the ever-increasing requirements for application in various fields.[27] To enhance the properties of polymers for application purposes, organic, ceramic and carbon-based fillers are either randomly dispersed, aligned or ordered in a multi-layer form in the polymer matrix.[15,20,22,25,27,33,36–38] In the last few years, among the various lead-free piezoceramics, barium calcium zirconium titanate (BCZT) with composition xBCT-(1-x) BZT has been widely explored for its piezoelectric and relaxor-type ferroelectric properties.[28,39,40] This system showed a maximum value of piezoelectric coefficient d_{33} of ≈ 620 pC/N in one of its composition (for $x = 0.5$).[41] Because of the high permittivity, good polarization and large energy density, the BCZT ceramics are also studied for energy storage purposes.[27,40,42,43] In this article, the as-synthesized BCZT ceramic particles with composition $0.5((Ba_{0.7}Ca_{0.3})TiO_3)–0.5(Ba(Zr_{0.2}Ti_{0.8})O_3)$ were dispersed in the PVDF matrix to enhance the electric properties of the polymer. The purpose is to integrate the enhanced electric properties of BCZT ceramic with the flexibility of PVDF polymer via a proper fabrication technique to form a suitable flexible electroactive material.[10,31,34]

Experimental Synthesis and Characterization

The BCZT source powder with composition $0.5((Ba_{0.7}Ca_{0.3})TiO_3)–0.5(Ba(Zr_{0.2}Ti_{0.8})O_3)$ was synthesized by sol-gel technique.[44] The precursor solution was formed using the starting materials of barium acetate ($Ba(CH_3COO)_2$) (LR grade purity), calcium nitrate tetrahydrate ($Ca(NO_3)_2·4H_2O$) (AR grade purity), zirconium oxychloride octahydrate ($ZrOCl_2·8H_2O$) (LR grade purity) and titanium isopropoxide (TTIP) as received without further purification.[33,45,46] Absolute ethanol and distilled water were used as solvents. Glacial acetic acid was added as a chelating agent.[45,46] On drying the precursor solution the obtained white solids were crushed and annealed at 1000°C for 4–5 h.[33,43,45,46]

Pure PVDF and PVDF/BCZT Composite Films

The fraction of α, β, and γ phases of PVDF in pure polymer and composite film samples depends on the synthesis technique and wt.% of dopant in the polymer matrix. To study the effect of synthesis technique and doping of as-synthesized BCZT nanoparticles, pure PVDF and PVDF/BCZT composite films with different wt.% of BCZT content were fabricated by solution-casting and melt-pressing.

a) Solution-Casting: Pure PVDF and PVDF/BCZT composite films with 10 wt.%, 20 wt.%, 30 wt.%, 40 wt.%, 50 wt.% and 60 wt.% of BCZT content were prepared by a solution-cast technique. The N,N-Dimethylformamide (DMF) was used as solvent to prepare PVDF solution.[33] The calculated amount of as-synthesized BCZT powder in proper wt.% ratio with PVDF was added to the polymer solution under continuous stirring. The mixture was sonicated several times for proper dispersion of ceramic particles. The prepared thick homogenous PVDF/BCZT mixture was then poured on a clean glass substrate and kept at 50°C overnight for drying. The as-prepared dried film was used for further analysis and testing.[9,18,25–27,33,43]

b) Melt-Pressing: For comparative studies of the processing temperature, pure PVDF and PVDF/BCZT composite films with 40 wt.%, 50 wt.% and 60 wt.% of BCZT were synthesized by melt-pressing. The BCZT powder and PVDF taken in different wt.% ratios were mixed and ground using a mortar and pestle. The mixed powder was placed between brass sheets in a stainless-steel die in a melt-press machine. The mixture was heated to 215°C and then a pressure of 250 kg/cm^2 was applied for 60 s. The die was cooled to room temperature slowly by flowing water through the heating platens. The sample film was pealed off carefully from the brass sheet and used for further analysis and testing.[47,48]

Characterization

A Fourier-transform infrared spectroscopy (FTIR) spectrophotometer (Spectrum Two, Perkin Elmer) was used to analyze the chemical structure of the sample films. The FTIR spectra of pure PVDF and PVDF/BCZT composite films were taken over a range of 450–1500^{-1} . An x-ray diffractometer (X'Pert Pro, PANalytical, Netherlands) with Cu-Kα radiation of wavelength $\lambda = 0.1540598$ nm was used to obtain the structural information of the sample films. The x-ray diffraction (XRD) data were collected over a range of $2\theta = 10°–80°$. To study the electric properties, Au-electrodes were sputtered using an automatic sputter coater (Agar Scientific, UK). The dielectric properties were analyzed using an impedance analyzer (Wayne Kerr, 6400B) over the frequency range of 20 Hz to 1 MHz at room temperature. The temperature-dependent dielectric properties were studied in the range 32–134°C at frequencies 100 Hz, 1 kHz, 10 kHz, 100 kHz and 1 MHz.

Results and Discussion

FTIR Spectroscopy

FTIR spectroscopy was used to analyze the chemical structure, and hence, the phase stabilization in the film samples. As explained earlier, PVDF is a semi-crystalline polymer which crystallizes into different structural polymorphs. In the α- and δ-phase, the chain conformations are designed as TGTG′ (T=trans, G=gauche$^+$, G′=gauche$^-$) and for β-phase are all trans, TTTT. However, for γ and ε the conformations are TTTGTTTG′, i.e. T$_3$GT$_3$G′.[9,10] The FTIR peaks in the range 876–885 cm^{-1}, 1067–1075 cm^{-1}, 1171–1182 cm^{-1}, and 1398–1404 cm^{-1} are common PVDF peaks that appear in all three phases (α, β, and γ).[8] The characteristic BCZT peak lies in the range 500–503 cm^{-1} of the spectra.[27] In pure PVDF film samples synthesized by solution-casting and melt-pressing, the

FTIR peaks corresponding to common PVDF peaks were all present in both the samples (Fig. 1a). In the PVDF film synthesized by solution-casting, the peaks at 1232 cm^{-1}, 834 cm^{-1}, and 478 cm^{-1} were the characteristic PVDF γ-phase peaks, while for the PVDF film synthesized by melt-pressing, the peaks at 762 (CF$_2$ bending and skeletal bending), 612 cm^{-1}, 486 cm^{-1} (CF$_2$ wagging), 528 cm^{-1}, 798 cm^{-1}, 976 cm^{-1}, 1150 cm^{-1}, and 1206 cm^{-1} were the characteristic PVDF α-phase peaks.[8,18,49] The peak at around 1276 cm^{-1} corresponds to the PVDF β-phase.

The FTIR data are generally normalized proportional to the thickness of samples for quantitative analysis. For pure PVDF film samples synthesized by solution-casting and melt-pressing, the FTIR data were normalized based on the transmittance peak at around 877 cm^{-1} as per the international standards (Fig. 1b).[50,51] The intensity of transmittance (%) peaks for all the common PVDF peaks were almost same for both the film samples. This reflects that the PVDF processing technique does not affect the overall crystallinity of the PVDF polymer matrix.

The PVDF/BCZT composite films having different wt.% of BCZT content synthesized by solution-cast and melt-press technique possessed the similar characteristic PVDF phase peaks as observed in pure PVDF film samples synthesized by the respective technique (Fig. 1c). The BCZT ceramic doping in the PVDF polymer matrix was found to have no significant effect on the structural conformation of PVDF.[52] For the composite films, the presence of BCZT in samples influenced the overall FTIR pattern, and the characteristic BCZT peak was present in the range 500–503 cm^{-1}. The FTIR pattern of composite films with different wt.% of BCZT content synthesized by the same technique was almost similar. The FTIR spectra of pure BCZT ceramic and PVDF/BCZT composite film with 50 wt.% BCZT content synthesized by solution-casting and melt-pressing has been compared (Fig. 1c). In the composite film samples fabricated by solution-casting, the PVDF peak at around 762 cm^{-1} (CF$_2$ bending and skeletal bending) was the characteristic α-phase peak whose intensity decreased with increasing BCZT content.[8] There was no peak at this position in the pure PVDF sample, i.e. the α-phase peak in the composite film arose due to the introduction of BCZT in PVDF polymer matrix whose intensity decreased with increasing BCZT content (Fig. S1).[27,49,52]

The normalized FTIR data of composite films with different wt.% of BCZT content fabricated by solution-casting and melt-pressing (Fig. 1d and e) revealed that the BCZT ceramic in PVDF affected the overall crystallinity of the polymer matrix.[52] It increased with an increase in BCZT content in the composite film. For films synthesized by solution-casting, it was maximum for 40 wt.% BCZT content composition. Similar results were reported earlier by analyzing XRD and DSC data. [49]
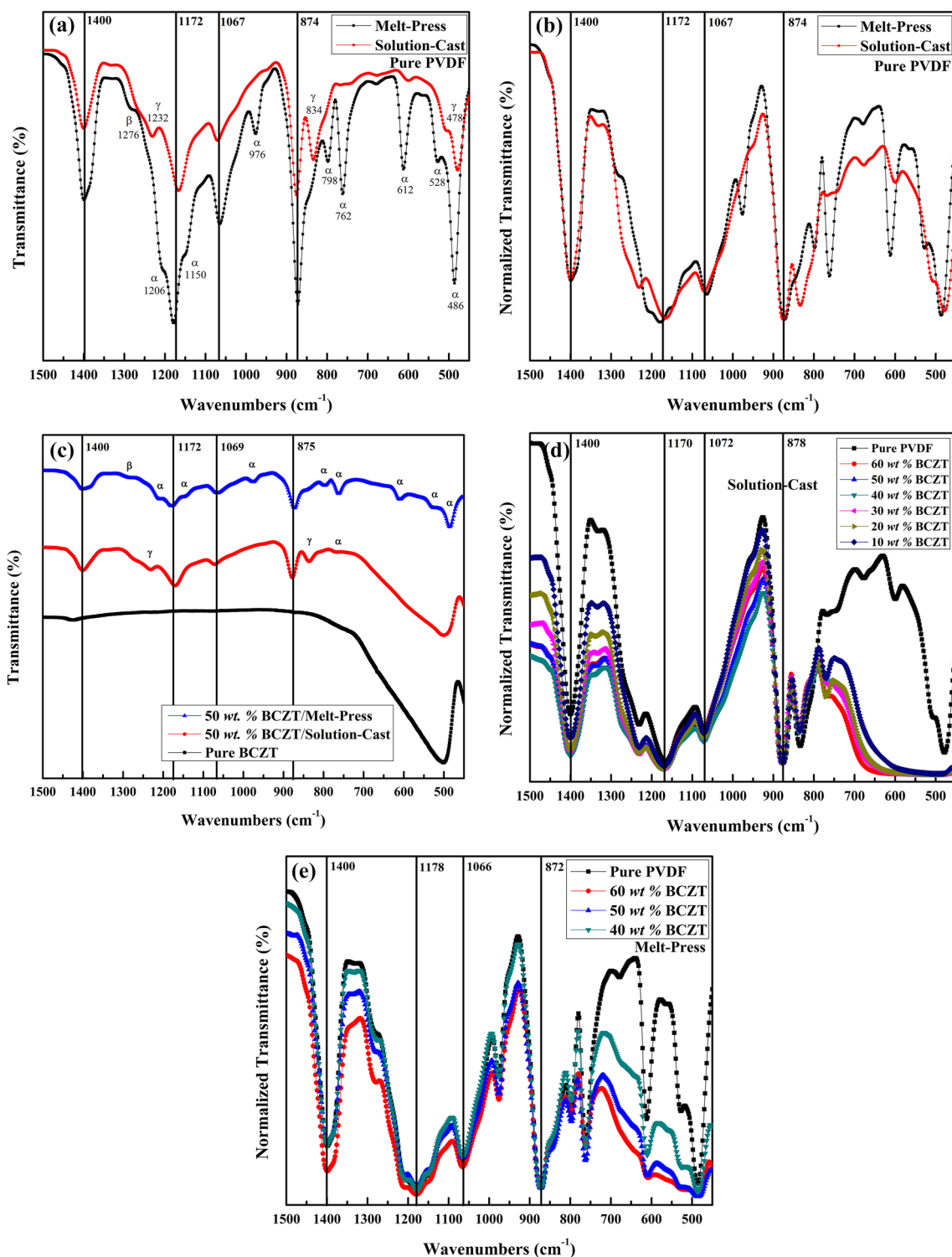
Fig. 1 (a) FTIR spectra in the range of 450–1500 cm^{-1} for pure PVDF film samples synthesized by solution-casting and melt-pressing (b) Normalized FTIR spectra in the range of 450–1500 cm^{-1} for pure PVDF films synthesized by solution-casting and melt-pressing (c) FTIR spectra in the range of 450–1500 cm^{-1} for pure BCZT powder and 50 wt.% BCZT content composite films synthesized by solu-tion-casting and melt-pressing (d) Normalized FTIR spectra in the range of 450–1500 cm^{-1} for pure PVDF and PVDF/BCZT composite films with different wt.% of BCZT content synthesized by solution-casting (e) Normalized FTIR spectra in the range of 450–1500 cm^{-1} for pure PVDF and PVDF/BCZT composite films with different wt.% of BCZT content synthesized by melt-pressing.

The FTIR spectroscopy results revealed that the polymer PVDF processed by solution-casting possessed γ-PVDF phase peaks while it stabilized mostly in the α-phase by melt-pressing.[5] Second, the BCZT ceramic particles in the PVDF matrix were found to have no significant effect on PVDF phase stabilization. However, it influenced the overall crystallinity of the polymer matrix.

X-Ray Diffraction (XRD) Studies

The structural analysis of as-synthesized BCZT powder, pure PVDF and composite films was done by x-ray diffraction (XRD). The XRD pattern of a pure PVDF film sample fabricated by melt-pressing (Fig. 2a) showed the presence of two intense peaks at around 18.4° and 20.0° corresponding to the α-phase of PVDF on the planes (020) and (110), respectively.[8,24,47,53] Along with these were the medium or weak peaks at 17.8°, 26.6° (021) and 35.9° (200) of α-PVDF. On the other hand, the XRD pattern of pure PVDF film prepared by solution-casting (Fig. 2a) exhibited a strong peak at 20.42° and two medium peaks around 18.52° and 39.24°, which correspond to diffraction peaks on planes (110/101), (020) and (211), respectively, of monoclinic γ-phase crystal. A medium diffraction peak around 36.23° was β-PVDF phase peak. The XRD results confirmed the formation of an α-phase and γ-phase with traces of a β-phase with melt-pressing and solution-casting, respectively.[5,8,18,24,27,43] These results were in good agreement with FTIR results of pure PVDF films.

The XRD pattern of 50 wt.% BCZT content composite films synthesized by solution-casting and melt-pressing displayed all the peaks corresponding to the pure BCZT phase and the similar characteristic PVDF phase peaks as observed in pure PVDF film samples synthesized by the respective technique (Fig. 2b). This indicates the incorporation of BCZT particles into the PVDF matrix without any secondary phase formation by both techniques.[49] The phase formation estimations were also in good agreement with FTIR analysis. In the XRD pattern of a composite film sample synthesized by solution-casting, peaks were less intense and the characteristic peaks of PVDF and BCZT were not well differentiated. This revealed that the BCZT ceramic particles were properly incorporated into the PVDF polymer matrix or polymer molecular chains properly covered the surface of ceramic particles in the samples prepared using solution-casting. Field emission scanning electron microscopy (FE-SEM) images of these samples also showed well-connected and uniformly distributed ceramic particles in the PVDF matrix.[54]

On the other hand, in the XRD pattern of the sample film fabricated by melt-pressing, the PVDF and BCZT characteristic peaks were well differentiated and intense. This showed that the polymer and ceramic particles were not mixed well/uniformly. SEM scans of the samples prepared using melt-pressing also revealed the non-uniformly distributed clusters of ceramic particles in the polymer matrix.[54] Moreover, the XRD pattern of a composite film prepared by solution-casting was slightly shifted towards a higher angle which might be due to the strain in the film. This could be due to the free-standing casting of the composite film prepared using solution-casting.[49,55]

Dielectric Properties

The dielectric permittivity of pure PVDF and PVDF/BCZT composite films was measured as a function of frequency in the range 20 Hz–1 MHz at room temperature. The dielectric permittivity of a medium depends on its electroactive
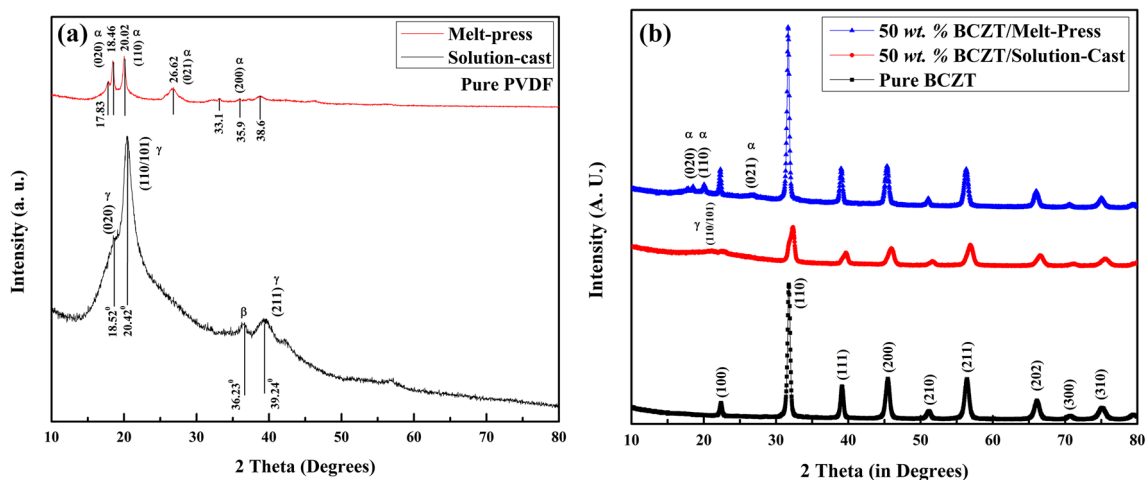

Fig. 2 (a) XRD pattern in the range of 10–80° for pure PVDF film samples synthesized by solution-casting and melt-pressing (b) XRD pattern in the range of 10–80° for pure BCZT powder and 50 wt.% BCZT content composite films synthesized by solution-casing and melt-pressing.

content and is related to the degree of polarization which includes all polarizations (electronic, ionic, orientational and interfacial).[27,33] The dielectric properties of multiphase PVDF are mostly related to their crystal structure which influence the polarity, portion of polar region and the freedom of molecular chains in the polar region.[24] The relative permittivity of pure PVDF film sample synthesized by solution-casting was measured to be ≈ 10 (at 120 Hz) which was comparatively more than the value of ≈ 7.5 (at 120 Hz) for the film synthesized by melt-pressing (Fig. 3a). As the phase stabilization was confirmed by FTIR and XRD studies, the dielectric studies showed that the γ-PVDF stabilized by solution-casting has higher polarity than α-PVDF stabilized by melt-pressing. This may be due to different chain conformations in two phases, i.e. (T$_3$GT$_3$G′) for γ-PVDF while (TGTG′) in α-PVDF. For PVDF/BCZT composite films, the resultant dielectric permittivity increased due to the introduction of ferroelectric BCZT ceramic powder and increase in interfacial interactions between BCZT ceramic particles and PVDF matrix.[36] The relative permittivity (ε_r) of composite films with 50 wt.% BCZT content synthesized by solution-casting and melt-pressing was ≈ 31 and 20 (at 120 Hz), respectively, which is about three times more than that of pure PVDF samples synthesized by the respective techniques (Table I).[49]

The dielectric loss of medium depends on polarization (dipolar, distortional and interfacial), i.e. loss due to bound charge and dipole relaxation phenomenon, and conduction loss due to dc electrical conduction.[27,33] For the pure PVDF film synthesized by melt-pressing the value of dielectric loss (tanδ) was found to be ≈ 0.35 (at 120 Hz) which was very large as compared to ≈ 0.07 (at 120 Hz) for the pure PVDF sample fabricated by solution-casting (Fig. 3b), i.e. the α-PVDF showed larger dielectric loss than γ-PVDF at low frequency (ranging 100 Hz to 10 kHz). When the test frequency was increased to 10 kHz, the electroactive
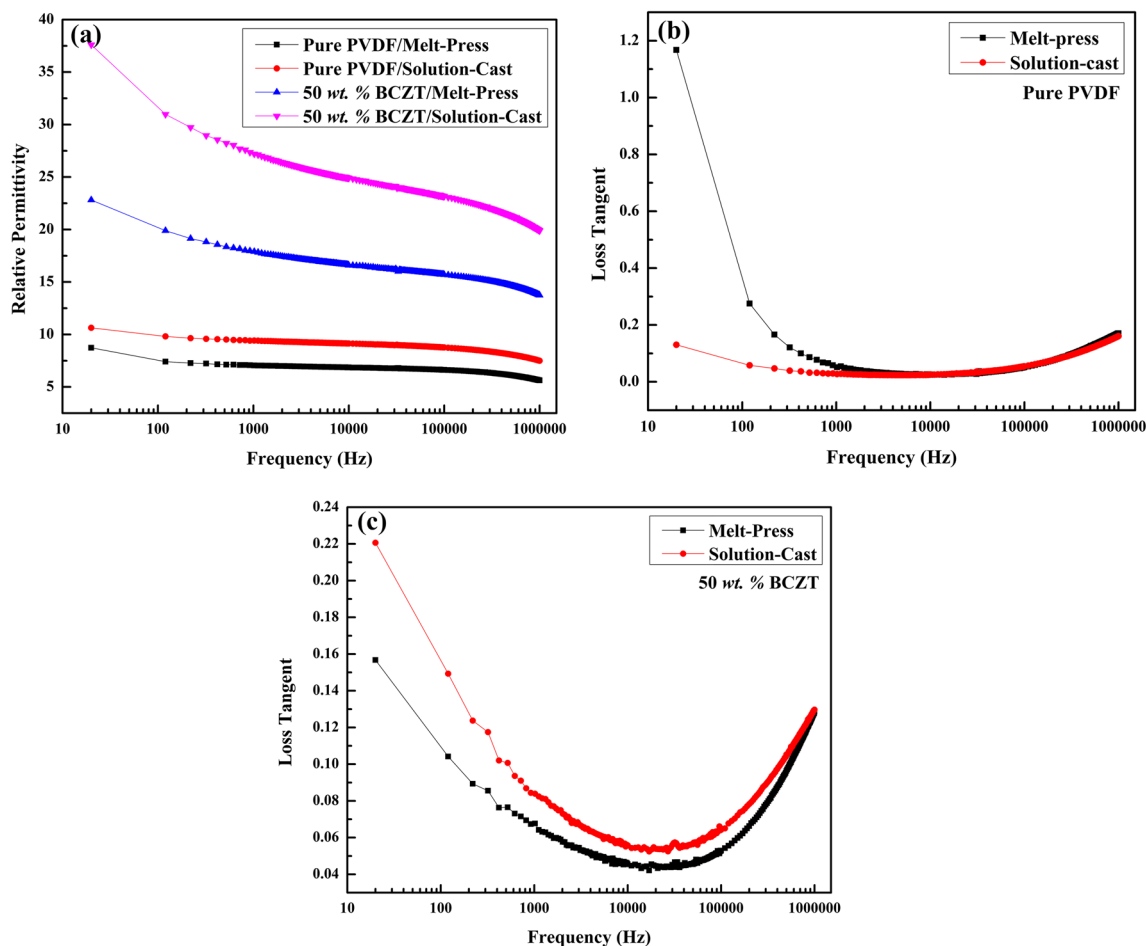

Fig. 3 (a) Variation of relative permittivity (ε_r) with frequency in the range 20 Hz–1 MHz for pure PVDF and 50 wt.% BCZT content composite films synthesized by solution-casting and melt-pressing (b) Variation of loss tangent (tanδ) with frequency in the range 20 Hz–1 MHz for pure PVDF films synthesized by solution-casting and melt-pressing (c) Variation of loss tangent (tanδ) with frequency in the range 20 Hz–1 MHz for 50 wt.% BCZT content composite films synthesized by solution-casting and melt-pressing.

Table I Value of relative permittivity (ε_r) and loss tangent (tanδ) of pure PVDF and 50 wt.% BCZT content composite films synthesized by solution-cast and melt-press techniques

Serial number	Sample	Electroactive phases	Relative permittivity ε_r (at 120 Hz)	Loss tangent tanδ (at 120 Hz)
1	Pure PVDF film (by solution-casting)	γ-PVDF	10	0.07
2	Pure PVDF film (by melt-pressing)	α-PVDF	7.5	0.35
3	PVDF/BCZT composite film with 50 wt.% BCZT content (by solution-casting)	γ-PVDF, BCZT ceramic	31	0.16
4	PVDF/BCZT composite film with 50 wt.% BCZT content (by melt-pressing)	α-PVDF, BCZT ceramic	20	0.11

γ-phase had slightly large dielectric loss. At higher frequencies, the dielectric loss for both phases increased obviously because of dielectric relaxation.[24] The addition of BCZT in PVDF introduced strong polarity groups derived from ionic polarization in its cell structure and also increased the charge accumulation at the interface of ceramic particles and PVDF matrix. This increased the overall polarization mechanism in composites. Moreover, with BCZT particles in the PVDF matrix, the long polymer chains were separated into smaller domains affecting the overall conductive network.[33] The loss tangent (tanδ) variation with frequency for composite films with 50 wt.% BCZT content synthesized by solution-casting and melt-pressing (Fig. 3c) confirmed the PVDF α-relaxation phenomenon in composites. At lower frequencies, the value of loss tangent (tanδ) was greater for the composite film synthesized by solution-casting. This may be due to the proper incorporation of BCZT ceramic particles in to the PVDF matrix by solution-casting as confirmed by XRD studies which led to significant increase in interfacial polarization and conduction loss due to formation of smaller domains of long polymeric chains, and hence, the higher tanδ value.[27,33,56] As the frequency increased, the difference in value of loss tangent decreased continuously and at one point, two curves coincided. This was due to the PVDF-α relaxation phenomenon at higher frequencies.

The variation of relative permittivity (ε_r) and loss tangent (tanδ) for pure PVDF and 50 wt.% BCZT content PVDF/BCZT composite films fabricated by solution-casting and melt-pressing were also studied with temperatures in the range 32–134°C at frequencies 100 Hz, 1 kHz, 10 kHz, 100 kHz and 1 MHz (Fig. 4). The increase in ε_r for composite films (Fig. 4b and d) is due to the increase in dipolar and interfacial polarization with the introduction of BCZT nanoparticles in the PVDF matrix. However, the low value of loss tangent (tanδ) for composites can be attributed to reduction in molecular dipoles with the decrease in wt.% of the PVDF matrix.[57]

For the pure PVDF film sample fabricated by solution-casting, a peak in variation of ε_r at ≈ 120°C corresponds to PVDF α-relaxation transition (Fig. 4a).[57,58] This could

be due to the wide-angle oscillations of dipoles attached to the main chain in the PVDF crystalline region and ferroelectric-paraelectric phase transition in PVDF at higher temperature.[59–61] The sudden decrease in ε_r and increase in tanδ above 130°C was due to melting of the polymer.[59] For the 50 wt.% BCZT content composite film fabricated by solution-casting, the characteristic PVDF α-relaxation peak was observed at around 120°C (Fig. 4b). In composites, the easier torsoinal and rotational movements of PVDF dipoles with field at higher temperature is significant as compared to BCZT nanoceramics.[57] Hence, the PVDF response was dominated in the overall dielectric relaxation phenomenon in composites. For the pure PVDF and 50 wt.% PVDF/BCZT composite film fabricated by melt-pressing, there was an increase in ε_r and tanδ at higher temperature during α-relaxation transition. However, no distinct peak was observed in both pure and composite film samples. This could be due to α-PVDF phase stabilization by melt-pressing while γ-PVDF stabilized in solution-cast films as confirmed by FTIR and XRD studies earlier.[62] At higher frequencies, a fluctuation in values was observed. This could be due to inhomogeneous dispersion and agglomeration of ceramic particles by melt-pressing.[52,54,56,63]

For the two different processing techniques, the results of FTIR, XRD and dielectric studies correlated and suggested that the pure PVDF film fabricated by solution-casting exhibited more PVDF electroactive phase content. Moreover, solution-casting is preferred due to its ease of control, low haze and low processing temperature requirements. With the progress in polymer sciences, a better understanding of the electric phenomenon in polymers has enabled a better design of polymer-based electroactive materials with desired/targeted properties for applications in flexible electronics.[1,2,29] Ceramic-polymer composites are the most promising material form in this regard. The ferroelectric PVDF/BCZT composites are widely studied for energy storage related applications.[1,2,29,43] The addition to BCZT particles in PVDF matrix has enhanced the electric response of the composite films which is most desirable in flexible electronics.
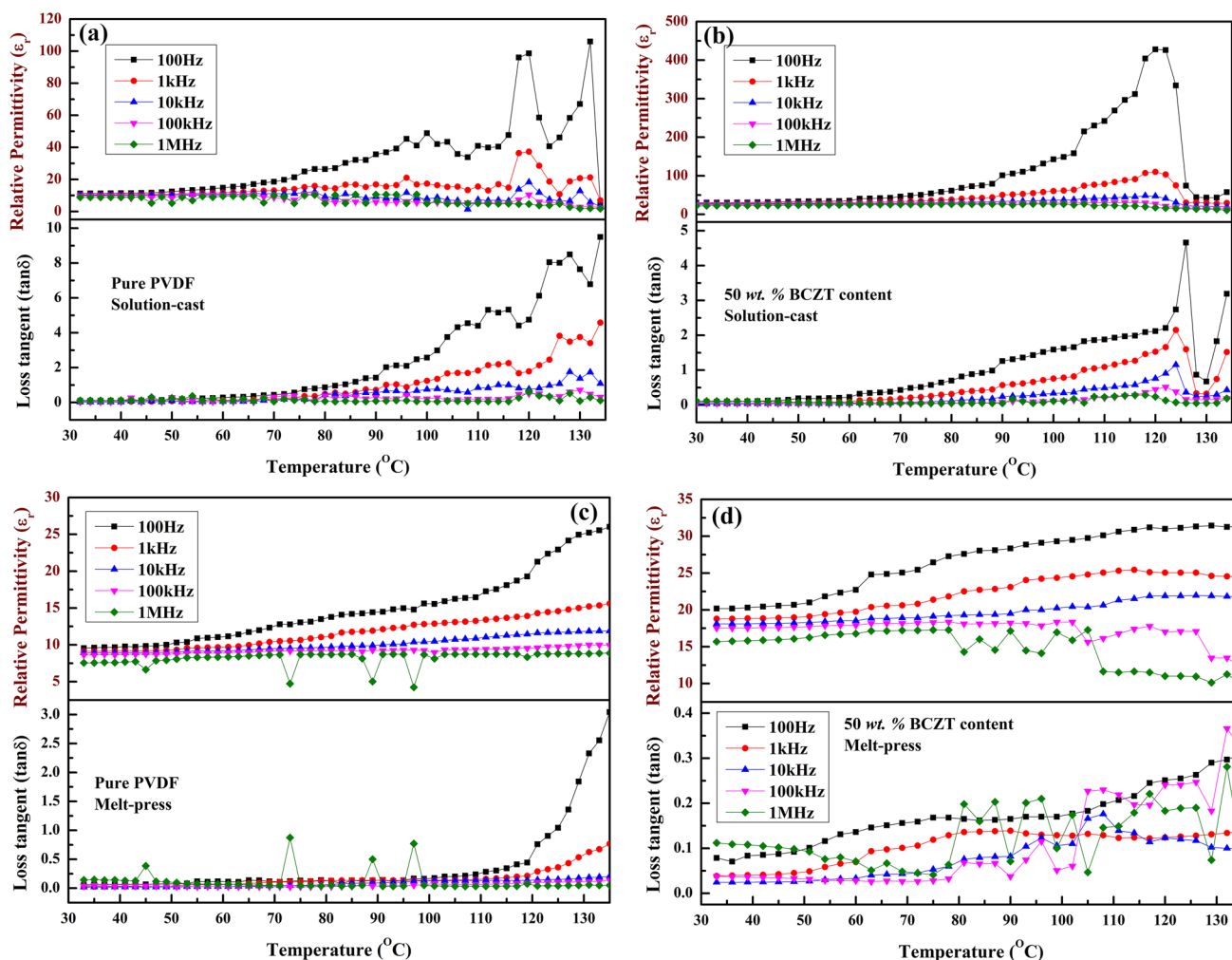
Fig. 4 Temperature-dependent variation of relative permittivity (ε_r) and loss tangent (tanδ) in the range 32–134°C at frequencies 100 Hz, 1 kHz, 10 kHz, 100 kHz and 1 MHz for (a) pure PVDF film fabricated by solution-casting (b) 50 wt.% BCZT content PVDF/BCZT composite film fabricated by solution-casting (c) pure PVDF film fabricated by melt-pressing, and (d) 50 wt.% BCZT content PVDF/BCZT composite film fabricated by melt-pressing.

Conclusions

1. The synthesis technique affected the PVDF molecular chain conformation during processing. Solution-casting involving softer synthesis conditions at low temperature ≈ 50°C stabilized PVDF mostly in the electroactive γ-phase. While high temperature (≈ 210°C) involved melt-pressing stabilized PVDF mostly in the α-phase.

2. The BCZT ceramic particles in composite film had no significant effect on PVDF phase stabilization. But it enhanced the overall crystallinity of the PVDF polymer matrix, and in this article, it was found to be maximal for 40 wt.% BCZT content film by solution-casting.

3. The relative permittivity (ε_r) of α-PVDF was less than γ-PVDF but the value of dielectric loss (tanδ) was very large for α-PVDF. With an addition of BCZT ceramic in the PVDF matrix, the ε_r of composite samples increased. This was because of an increase in dipolar and interfacial polarizations in the composites.

4. The γ-PVDF stabilized in pure and composite film samples fabricated by solution-casting showed a distinct PVDF-α relaxation peak at ≈ 120°C and polymer melting at temperature > 130°C. Meanwhile, for α-PVDF stabilized by melt-pressing, there was an increase in ε_r and tanδ at higher temperature during α-relaxation transition.

References

1. H. Kawai, *Jpn. J. Appl. Phys.* 8, 975 (1969).
2. A.J. Lovinger, *Science* 220, 1115 (1983).
3. P. Martins, A.C. Lopes, and S. Lanceros-Mendez, *Prog. Polym. Sci.* 39, 683 (2014).
4. K.S. Ramadan, D. Sameoto, and S. Evoy, *Smart Mater. Struct.* 23, 1 (2014).
5. M. Li, H.J. Wondergem, M.-J. Spijkman, K. Asadi, I. Katsouras, P.W.M. Blom, and D.M. de Leeuw, *Nat. Mater.* 12, 433 (2013).
6. Z. Cui, N.T. Hassankiadeh, Y. Zhuang, E. Drioli, and Y.M. Lee, *Prog. Polym. Sci.* 51, 94 (2015).
7. F. Liu, N.A. Hashim, Y. Liu, M.R.M. Abed, and K. Li, *J. Memb. Sci.* 375, 1 (2011).
8. X. Cai, T. Lei, D. Sun, and L. Lin, *RSC Adv.* 7, 15382 (2017).
9. M.G. Buonomenna, P. Macchi, M. Davoli, and E. Drioli, *Eur. Polym. J.* 43, 1557 (2007).
10. N.A. Hoque, P. Thakur, S. Roy, A. Kool, B. Bagchi, P. Biswas, M.M. Saikh, F. Khatun, S. Das, and P.P. Ray, *MACS Appl. Mater. Interfaces* 9, 23048 (2017).
11. H. Wang, Q. Chen, W. Xia, X. Qiu, Q. Cheng, and G. Zhu, *J. Appl. Polym. Sci.* 135, 46324 (2018).
12. L. Li, M. Zhang, M. Rong, and W. Ruan, *RSC Adv.* 4, 3938 (2014).
13. S.P. Muduli, S. Parida, S.K. Rout, S. Rajput, and M. Kar, *Mater. Res. Express* 6, 095306 (2019).
14. I.O. Pariy, A.A. Ivanova, V.V. Shvartsman, D.C. Lupascu, G.B. Sukhorukov, M.A. Surmeneva, and R.A. Surmenev, *Mater. Chem. Phys.* 239, 122035 (2020).
15. T. Men, X. Liu, B. Jiang, X. Long, and H. Guo, *Thin Solid Films* 669, 579 (2019).
16. V.K. Tiwari, Y. Lee, G. Song, K. Lib Kim, Y. Jung Park, and C. Park, *J. Polym. Sci. Part B Polym. Phys.* 56, 795 (2018).
17. S. Yang, F. Wang, X. Li, Y. Wu, T. Chang, Z. Hu, and G. An, *Polymer (Guildf)* 181, 121784 (2019).
18. S.K. Karan, S. Maiti, A.K. Agrawal, A.K. Das, A. Maitra, S. Paria, A. Bera, R. Bera, L. Halder, A.K. Mishra, J.K. Kim, and B.B. Khatua, *Nano Energy* 59, 169 (2019).
19. S.-H. Kim, S.-J. Park, C.-Y. Cho, H.S. Kang, E.-H. Sohn, I.J. Park, J.-W. Ha, and S.G. Lee, *RSC Adv.* 9, 40286 (2019).
20. P. Thakur, A. Kool, N.A. Hoque, B. Bagchi, F. Khatun, P. Biswas, D. Brahma, S. Roy, S. Banerjee, and S. Das, *Nano Energy* 44, 456 (2018).
21. A. Gebrekrstos, G. Prasanna Kar, G. Madras, A. Misra, and S. Bose, *Polymer (Guildf)* 181, 121764 (2019).
22. N.A. Shepelin, A.M. Glushenkov, V.C. Lussini, P.J. Fox, G.W. Dicinoski, J.G. Shapter, and A.V. Ellis, *Energy Environ. Sci.* 12, 1143 (2019).
23. P. Thakur, A. Kool, N.A. Hoque, B. Bagchi, S. Roy, N. Sepay, S. Das, and P. Nandy, *RSC Adv.* 6, 26288 (2016).
24. W. Xia, and Z. Zhang, *IET Nanodielectrics* 1, 17 (2018).
25. S. Amiri, and A. Rahimi, *Iran. Polym. J. (English Ed.)* 25, 559 (2016).
26. U. Siemann, *Prog. Colloid Polym. Sci.* 130, 1 (2005).
27. H. Lu, L. Liu, J. Lin, W. Yang, L. Weng, X. Zhang, G. Chen, and W. Huang, *J. Appl. Polym. Sci.* 134, 45362 (2017).
28. M.E. Villafuerte-Castrejón, E. Morán, A. Reyes-Montero, R. Vivar-Ocampo, J.-A. Peña-Jiménez, S.-O. Rea-López, and L. Pardo, *Materials (Basel, Switzerland)* 9, 21 (2016).
29. Q. Li, and Q. Wang, *Macromol. Chem. Phys.* 217, 1228 (2016).
30. M. Bashir, and P. Rajendran, *J. Intell. Mater. Syst. Struct.* 29, 3681 (2018).
31. B. Stadlober, M. Zirkl, and M. Irimia-Vladu, *Chem. Soc. Rev.* 48, 1787 (2019).
32. H.B. Jung, J.W. Kim, J.H. Lim, D.K. Kwon, D.H. Choi, and D.Y. Jeong, *Electron. Mater. Lett.* 16, 47 (2019).
33. A. Patra, A. Pal, and S. Sen, *Ceram. Int.* 44, 11196 (2018).
34. X. Chen, X. Han, and Q.-D. Shen, *Adv. Electron. Mater.* 3, 1600460 (2017).
35. B. Chu, X. Zhou, K. Ren, B. Neese, M. Lin, Q. Wang, F. Bauer, and Q.M. Zhang, *Science* 313, 334 (2006).
36. H. Luo, X. Zhou, C. Ellingford, Y. Zhang, S. Chen, K. Zhou, D. Zhang, C.R. Bowen, and C. Wan, *Chem. Soc. Rev.* 48, 4424 (2019).
37. V.K. Thakur, and R.K. Gupta, *Chem. Rev.* 116, 4260 (2016).
38. M. Guo, J. Jiang, Z. Shen, Y. Lin, C.W. Nan, and Y. Shen, *Mater. Today* 29, 49 (2019).
39. C.-H. Hong, H.-P. Kim, B.-Y. Choi, H.-S. Han, J.S. Son, C.W. Ahn, and W. Jo, *J. Mater.* 2, 1 (2016).
40. A.R. Jayakrishnan, K.V. Alex, A. Thomas, J.P.B. Silva, K. Kamakshi, N. Dabra, K.C. Sekhar, J. Agostinho Moreira, and M.J.M. Gomes, *Ceram. Int.* 45, 5808 (2019).
41. W. Liu, and X. Ren, *Phys. Rev. Lett.* 103, 257602 (2009).
42. M. Peddigari, H. Palneedi, G.T. Hwang, and J. Ryu, *J. Korean Ceram. Soc.* 56, 1 (2019).
43. T. Garg, V. Annapureddy, K.C. Sekhar, D. Jeong, N. Dabra, and J.S. Hundal, *Polym. Compos.* 41, 5305 (2020).
44. G. Pfaff, *J. Mater. Chem.* 2, 591 (1992).
45. Z. Wang, K. Zhao, X. Guo, W. Sun, H. Jiang, X. Han, X. Tao, Z. Cheng, H. Zhao, H. Kimura, G. Yuan, J. Yin, and Z. Liu, *J. Mater. Chem. C* 1, 522 (2013).
46. J.P. Praveen, T. Karthik, A.R. James, E. Chandrakala, S. Asthana, and D. Das, *J. Eur. Ceram. Soc.* 35, 1785 (2015).
47. A.V. Reddy, K.C. Sekhar, N. Dabra, A. Nautiyal, J.S. Hundal, N.P. Pathak, and R. Nath, *ISRN Mater. Sci.* 2011, 1 (2011).
48. N. Kumar, N. Dabra, J.S. Hundal, and R. Nath, *Ferroelectr. Lett. Sect.* 40, 108 (2013).
49. M. Sharma, J.K. Quamara, and A. Gaur, *J. Mater. Sci. Mater. Electron.* 29, 10875 (2018).
50. K. Tashiro, M. Kobayashi, and H. Tadokoro, *Macromolecules* 14, 1757 (1981).
51. H.S. Mohanty, A. Kumar, P.K. Kulriya, R. Thomas, and D.K. Pradhan, *Mater. Chem. Phys.* 230, 221 (2019).
52. A.N. Arshad, M.H.M. Wahid, M. Rusop, W.H.A. Majid, R.H.Y. Subban, and M.D. Rozana, *J. Nanomater.* 2019, 1 (2019).
53. L. Ruan, X. Yao, Y. Chang, L. Zhou, G. Qin, and X. Zhang, *Polymers (Basel)* 10, 1 (2018).
54. T. Garg, N. Dabra and J.S. Hundal, Proceedings of the National Conference on Materials Science (2021) Communicated.
55. T.S. Chow, C.A. Liu, and R.C. Penwell, *J. Polym. Sci. Polym. Phys. Ed.* 14, 1311 (1976).
56. M. Bhattacharya, *Materials (Basel)* 9, 262 (2016).
57. J. Fu, Y. Hou, M. Zheng, Q. Wei, M. Zhu, and H. Yan, *ACS Appl. Mater. Interfaces* 7, 24480 (2015).
58. H. Rekik, Z. Ghallabi, I. Royaud, M. Arous, G. Seytre, G. Boiteux, and A. Kallel, *Compos. Part B Eng.* 45, 1199 (2013).
59. B. Hilczer, H. Smogór, and J. Goslar, *J. Mater. Sci.* 41, 117 (2006).
60. Z.M. Dang, L. Wang, H.Y. Wang, C.W. Nan, D. Xie, Y. Yin, and S.C. Tjong, *Appl. Phys. Lett.* 86, 1 (2005).

61. A. Pramanick, S. Misture, N.C. Osti, N. Jalarvo, S.O. Diallo, and E. Mamontov, *Phys. Rev. B* 96, 174103 (2017).
62. E. Ozkazanc, and H.Y. Guney, *J. Appl. Polym. Sci.* 112, 2482 (2009).
63. F. Bensadoun, N. Kchit, C. Billotte, F. Trochu, and E. Ruiz, *J. Nanomater.* 2011, 1 (2011).

Publisher's Note Springer Nature remains neutral with regard to jurisdictional claims in published maps and institutional affiliations.